ELSEVIER

Journal of Nuclear Materials 290–293 (2001) 286–290

journal of nuclear materials

www.elsevier.nl/locate/jnucmat

Molybdenum sources and transport in Alcator C-Mod

B. Lipschultz *, D.A. Pappas, B. LaBombard, J.E. Rice, D. Smith, S. Wukitch

Massachusetts Institute of Technology, Plasma Science and Fusion Center Room NW 17-103, 77 Massachusetts Avenue, Cambridge, MA 02139, USA

Abstract

We present a characterization of molybdenum sources, Γ_{Mo}, core Mo content, N_{Mo}, and their dependencies on Alcator C-Mod operational regimes. This includes sources from the divertor, the inner wall and the ICRF antenna limiters. We also present information characterizing the penetration of these impurities into the core plasma under different conditions based on penetration factors, $PF = N_{Mo}/\Gamma_{Mo}$ (s). In general, the inner wall Mo source is large ($\sim 10^{18}$ s^{-1}) but is found to be relatively uncorrelated with the core Mo level in diverted plasmas. The outer divertor source is of similar order to that from the inner wall and has a penetration factor in the range 10^{-5}–2×10^{-3} s depending on density and confinement mode. The antenna limiter Mo sources are typically smaller, but with higher penetration factors – 10^{-3}–2×10^{-2} s. The behavior of the antenna limiter sources is consistent with physical sputtering due to the influence of RF sheath rectification. © 2001 Elsevier Science B.V. All rights reserved.

Keywords: High-Z material; Impurity screening; Impurity source; Alcator C-Mod

1. Introduction

The impurity content of the plasma core is an important factor in determining the success of any fusion experiment. As part of the effort to predict impurity levels it is important to understand the processes of impurity generation, transport in the SOL and in the core. The effects of the type of operation (limited versus diverted) and confinement mode (L- or H-mode) on transport are important factors as well.

High-Z materials are envisaged for use as part of the first-wall in a magnetic fusion reactor (instead of, for example, carbon) because of erosion, hydrogen retention and safety concerns [1]. Studies of high-Z sources have been performed on limiter [2–5] and divertor tokamaks [6–9]. The issue of impurity penetration to the core has often been separately addressed through examination of recycling [10–13] and non-recycling elements [11,12,14–18]. The experience with high-Z materials has not been as prevalent as that with carbon, particularly in the presence of RF heating. In this paper, we characterize the experience with Mo sources and their penetration to the core plasma in Alcator C-Mod, a divertor tokamak.

2. Experiment and technique

Basic characteristics of the Alcator C-Mod experiment and diagnostics are described elsewhere [19]. The plasma discharges studied had a 5.3 T toroidal field and plasma currents in the range 0.8–1.0 MA. All discharges were diverted with a single field null at the bottom of the machine. The data in this study are primarily from ICRF-heated discharges (both L- and H-mode) using two-strap antennas launching waves at 80 MHz [19].

The plasma-interaction surfaces of the tokamak are all molybdenum tiles with boronization conditioning. This includes the inner vessel wall and the lower divertor. In addition, for protection of the antennas there are partial poloidal limiters at the outside edge of the plasma as well as tiles directly attached to the outside edge of the antennas, forming a 'picture frame'. The poloidal limiter is typically located ~1 cm radially outside the separatrix (referenced to the midplane). The antenna protection tiles and Faraday screen are located 0.5 and 1.0 cm, further away from the core plasma.

* Corresponding author: Tel.: +1 617 253 8636; fax: +1 617 253 0627.

E-mail address: blip@psfc.mit.edu (B. Lipschultz).

0022-3115/01/$ - see front matter © 2001 Elsevier Science B.V. All rights reserved.
PII: S0022-3115(00)00436-0

The Mo influx is based on measurements of the Mo-I line brightness at 386.4 nm. Fiber optics are employed to relay the light collected by a number of imaging systems viewing different first-wall surfaces around the vessel to an $f/4$, 0.25 m visible spectrometer which simultaneously monitors 16 of those locations. The inverse photon efficiency for the Mo-I line is utilized to convert the Mo-I photon brightness to influx (per unit area) based on a standard formalism [15]. The n_e and T_e in the SOL and at the plate needed for determination of inverse photon efficiencies are measured by Langmuir probes [20]. Multiplication of the influx by source area gives the total source flux, Γ_{Mo}. The core Mo content is determined from the brightness of a Mo^{33+} line at 0.3740 nm and modeling using the core n_e and T_e profiles [21].

The general concept of penetration factor, PF, has been defined previously [16,12] as the ratio of a given core impurity level, N_Z, to its corresponding source, Γ_Z at the first wall ($PF = N_Z/\Gamma_Z$). The relationship between the probability that an impurity neutral will enter the core, η_Z, and PF is defined as $\eta_Z = PF/\tau_Z$, where τ_Z is the core impurity confinement time [13].

3. Source characterization

The most important Mo sources are the outer divertor, sections of the inner wall near the midplane and, for ICRF-heated discharges, the antenna protection limiters. Fig. 1 illustrates the relative strengths of the relevant sources and the variations that can occur during a single shot. The plasma switches from being limited on the inner wall to diverted near the beginning and end of the shot (separatrix to inner-wall gap, Fig. 1(b)). The ICRF power is on from 0.5 to 1.2 s, Fig. 1(b). The core confinement switches from L- to H-mode at ~0.92 s, as evidenced by the rise in core density Fig. 1(a). Note that this particular H-mode is ELM-free, which not only leads to increased energy confinement, but also leads to impurity accumulation.

Of primary interest is the core Mo level shown in Fig. 1(e). It is highest during the period when the plasma is limited on the inner wall and drops as the plasma becomes diverted. The core Mo levels increase again when RF power is injected, further increasing when the plasma energy confinement changes from L- to H-mode. The core Mo level would rise during H-mode even if the Mo source rate stays constant, given that the impurity confinement increases [22]. The inner wall source, Fig. 1(d), is largest during the period when the plasma is limited and then steadily decreases throughout most of the shot, dropping dramatically during the ELM-free phase. The lack of correlation between wall source and core content seen in this figure is typical for diverted plasmas, even though the wall source is of similar order or larger than other sources.

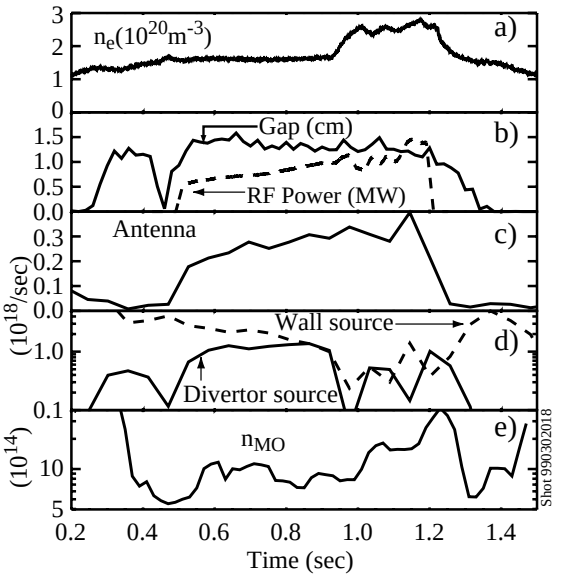

Fig. 1. Discharge parameters: (a) $\bar{n}_e$; (b) separatrix to inner-wall gap and ICRF power; (c) Mo source rate from the antenna limiter; (d) Mo source rate from outer divertor and inner wall; and (e) core N_{Mo}. H-mode starts and ends at ~0.93 and 1.23 s, respectively.

The core Mo levels are more correlated to the outer divertor source, Fig. 1(d). Again referring to Fig. 1, the divertor Mo source increases as the plasma becomes diverted, with a second increase following injection of RF power. Interestingly, the outer divertor source also decreases during the ELM-free H-mode period. This drop in Mo source rate for the divertor and inner wall is correlated with the observed decrease in power flow to the divertor (and thus, the SOL) during ELM-free H-modes.

The clearest correlation between a Mo source and the core Mo level is that of the antenna, Fig. 1(c). It rises when the RF power is injected, increases proportionally to the RF power and then returns to insignificant levels after the RF is off. The magnitude of the antenna source is less than that from the inner wall and divertor.

To explore the correlation between the antenna source and core Mo content further, we refer to Fig. 2. The impurity confinement and core $\bar{n}_e$ are held constant in these L-mode discharges. The wall source was essentially constant, again showing lack of correlation with the core Mo levels. The core Mo level and the antenna Mo source rate rise linearly with RF power, increasing by factors of 6–8. The outer divertor Mo source initially increases more slowly as a function of RF power, increasing more rapidly at higher RF powers.

The plasma density also appears to be an important factor as seen in Figs. 3(a)–(c). Although there is significant scatter in the data, due primarily to the

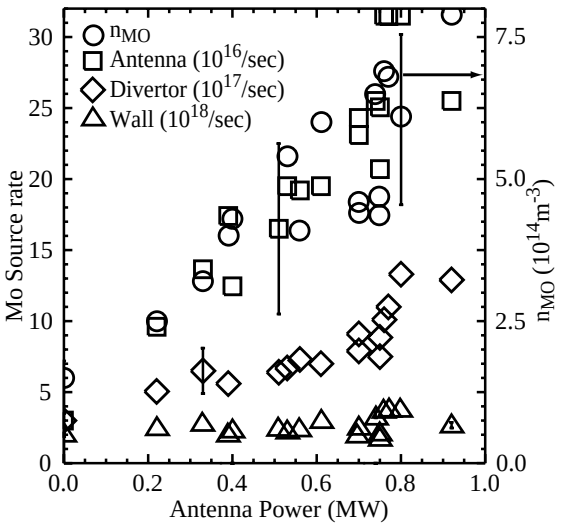

Fig. 2. Variation of Mo sources with ICRF power for a series of L-mode discharges at $\bar{n}_e \sim 2.0 \times 10^{20}$ m^{-3}.

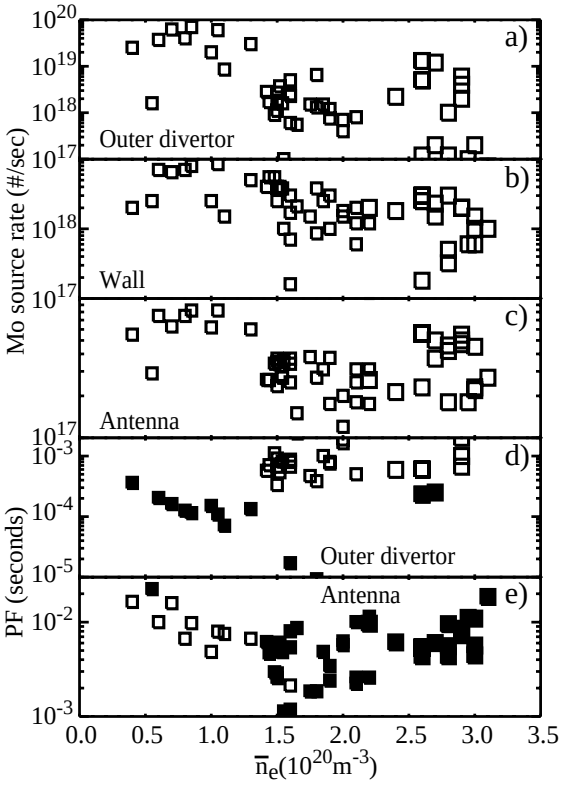

Fig. 3. Variation in Mo sources (a)–(c) and PF (d),(e) versus $\bar{n}_e$. H-mode cases have the larger symbols. Cases where a particular source (e.g., antenna protection tiles) is dominant are shaded.

variations in RF power, there is a trend for all sources to decrease with increasing density. The fractional decrease is largest for the divertor which, although the largest at low densities, drops to levels approaching the antenna source rate at densities around 1.5×10^{20} m^{-3}. At densities above 2.0×10^{20} m^{-3} the plasmas are in H-mode. This appears generally to increase the sources, but these data are quite scattered.

4. Source dominance

We can perhaps shed some light on the relative contribution to the core N_{Mo} by different sources through examination of the penetration factor for the outer divertor (PF_{OD}) and antenna (PF_{ANT}) as seen in Figs. 3(d) and (e). Note that we use the *total* core Mo level in calculating each PF. The calculated PF is thus, an upper bound. In general, PF_{ANT} is considerably higher than PF_{OD}, except for densities above 1.5×10^{20} m^{-3}. In addition, the lowest PFs for antenna and outer divertor sources *are almost 2 orders of magnitude apart.*

The shots included in this database have been examined for variations in source rates and core levels, such as that shown in Fig. 1, in order to determine which data points are from discharges where N_{Mo} appears to be dominated by either the antenna or outer-divertor. Based on that subjective analysis the antenna source 'dominates' over that of the outer divertor for cases where $\Gamma_{ANT}/\Gamma_{OD} > 0.1$. The filled datapoints of Figs. 3(d) and (e) represent such cases of divertor (3(d)), and antenna (3(e)) dominance. Wall penetration data is not included here because of the lack of correlation with core Mo (very low PF).

5. Discussion

The penetration factors obtained where one source or the other is 'dominant' are reasonable in comparison to past work at Alcator C-Mod. Mo is a non-recycling impurity and thus, the closest comparison is to penetration data obtained with N_2 and CH_4 [17]. For a series of discharges with $\bar{n}_e \sim 1.3$–1.8×10^{20} m^{-3}, the inner wall was determined to have the lowest PF. The PF values for divertor gas injection were in the range 10^{-5}–2×10^{-3} s. The PF values for injection of gas from the outer midplane were higher, 10^{-3}–2×10^{-2} s. These PFs are similar to the data in Figs. 3(d) and (e). The ionization mean free paths for Mo and N are close (~2 versus 6 mm near the antenna) so that impurity neutrals are ionized far from the separatrix. Thus, transport which we do not expect to be very different for these elements, determines the level in the core.

As mentioned in Section 1, one can extract information about impurity screening from PF using knowledge of τ_Z. Typical values of τ_Z in C-Mod are ~20 ms, and 20–200 ms for L- and EDA H-modes,

respectively. The resultant η_{ANT} is 5–100% for L-mode and 2–10% for EDA H-modes. The outer divertor η_{OD} are 0.1–1.5% in L-mode and 0.1–1.0% in EDA H-modes. The screening of antenna-generated Mo is of similar magnitude to that obtained from laser-blowoff of Sc at the midplane [23]. As seen in previous work [16,17] the divertor Mo source is much better screened than that from the antenna, although in this study the ratio η_{ANT}/η_{OD} tends to be slightly larger.

The question arises as to why the antenna protection tiles are such a significant source of impurities. The poloidal limiters, mentioned earlier, are 5 mm closer to the separatrix and yet are not significant Mo source locations. When the SOL heat flux is reduced during ELM-free H-modes the outer divertor and inner wall sources drop, but the antenna source, which is at larger minor radii, does not. *In fact, it stays proportional to the ICRF power*. The plasma in the region of the antenna has much lower densities than the outer divertor (1×10^{19} m^{-3} versus 1–10×10^{20} m^{-3}), similar plasma temperatures (10 eV) and much smaller Mo emission area. Thus, one would expect the antenna source to be negligible compared to the divertor. All these differences point towards the possibility that different mechanisms are in play at the antenna, most likely due to the presence of ICRF. As a working hypothesis, we point towards previous work with ICRF where sheath-rectification, leading to enhanced plasma potentials and sputtering, was identified as the cause of impurity generation [24]. We examine this effect in C-Mod by measuring the floating potential, V_F, and T_e profiles and utilizing their relationship to the plasma potential, $V_P = V_F + \sim 3xT_e$, Fig. 4. The addition of RF with standard heating phasing (0:π) raises V_P by 10's of volts on field lines connected to the antenna protection tiles. The potential is increased further with poor phasing (0:0.3π). Increased plasma potentials would lead to increased sputtering. Further work is needed to determine the validity of this working hypothesis.

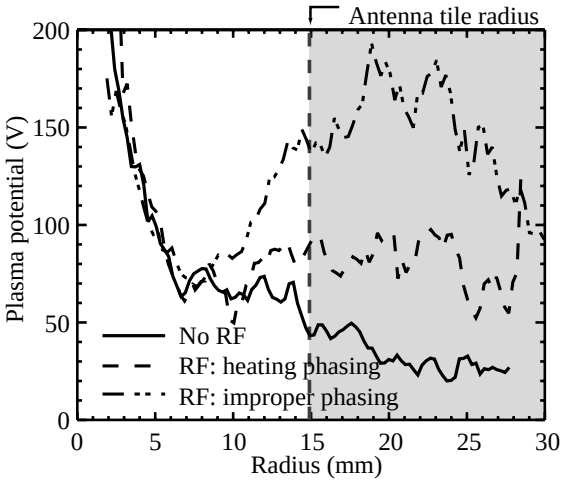

Fig. 4. Plasma potential in the SOL inferred from Langmuir probe measurements for cases with and without ICRF.

6. Summary

The primary source locations for Mo which affect diverted discharges are the outer divertor, the inner wall and the ICRF antenna protection limiters. Depending on plasma density, level of injected RF power and the confinement mode, different source locations appear to dominate the core Mo levels. In general, the inner wall Mo source is large ($\sim 10^{18}$ s^{-1}) but is found to be relatively uncorrelated with the core level of Mo in diverted plasmas. The outer divertor source is of similar order to that from the inner wall and has a penetration factor in the range 10^{-5}–2×10^{-3} s, the highest for the low densities and H-modes. The antenna tile Mo sources are typically smaller, but with higher penetration factors – 10^{-3}–2×10^{-2} s having a dependence on density and confinement mode similar to the divertor sources. The penetration factors from the different locations are consistent with that obtained previously with non-recycling gases; divertor sources are better screened from the core. The behavior of the antenna limiter sources is consistent with physical sputtering due to the influence of RF sheath rectification. Screening efficiencies for the different locations are estimated based on core impurity confinements times. They scale the same, in terms of location and density, as the penetration factors.

Acknowledgements

The authors wish to thank the entire Alcator group for assistance in acquiring this data. The authors gratefully acknowledge helpful discussions with G.M. McCracken, C.S. Pitcher and J.L. Terry. This work was supported by the US Department of Energy under grant DE-FC02-99ER54512.

References

[1] ITER expert group on divertor physics et al., Nucl. Fus. 39 (1999) 2391.
[2] B. Lipschultz, B. LaBombard, E.S. Marmar et al., J. Nucl. Mater. 128&129 (1984) 555.
[3] J.E. Rice, E.S. Marmar, B. Lipschultz, J.L. Terry, Nucl. Fus. 24 (1984) 329.
[4] V. Philips, M. Tokar, A. Pospieszczyk et al., in: Proceedings of the 22nd European Conference on Control Fusion and Plasma Physics, Bournemouth, UK, July 1995, Paper II, 321.

[5] B. Unterberg, H. Knauf, P. Lindner et al., J. Nucl. Mater. 241–243 (1997) 793.
[6] A.R. Field, G. Fussmann, C. Garcia-Rosales et al., J. Nucl. Mater. 220–222 (1995) 553.
[7] A. Thoma, K. Asmussen, R. Dux et al., Plasma Phys. Cont. Fus. 39 (1997) 1487.
[8] K. Krieger, J. Roth, A. Annen et al., J. Nucl. Mater. 241–243 (1997) 684.
[9] D.A. Pappas, B. Lipschultz, B. LaBombard et al., J. Nucl. Mater 266–269 (1999) 635.
[10] C. Belanger, B.C. Gregory, E. Haddad et al., Nucl. Fus. 31 (1991) 561.
[11] G.M. McCracken, U. Samm, P.C. Stangeby, Nucl. Fus. 33 (1993) 1409.
[12] G.M. McCracken, R.S. Granetz, B. Lipschultz et al., J. Nucl. Mater. 241–243 (1997) 788.
[13] R.S. Granetz, G.M. McCracken, F. Bombarda, J. Nucl. Mater. 241–243 (1997) 788.
[14] J. Roth, G. Janeschitz, Nucl. Fus. 29 (1989) 915.
[15] G. Fussmann, J.V. Hofmann, G. Janeschitz et al., Nucl. Fus. 30 (1990) 2319.
[16] G. Janeschitz, R. Konig, L. Lauro-Taroni et al., J. Nucl. Mater. 196–198 (1992) 380.
[17] G.M. McCracken, B. Lipschultz, B. LaBombard et al., Phys. Plasmas 4 (1997) 1681.
[18] D. Whyte, B.C. Gregory, G. Abel et al., Nucl. Fus. 34 (1994) 203.
[19] I.H. Hutchinson et al., Phys. Plasmas 1 (1994) 1511.
[20] B. LaBombard et al., Phys. Plasmas 2 (1995) 2242.
[21] J.E. Rice, J.L. Terry, K.B. Fournier et al., J. Phys. B 29 (1996) 2191.
[22] J.E. Rice, J.L. Terry, J.A. Goetz et al., Phys. Plasmas 4 (1997) 1605.
[23] M.A. Graf, J.E. Rice, J.L. Terry et al., Rev. Sci. Instrum. 66 (1995) 636.
[24] R. Majeski, P.H. Probert, T. Tanaka et al., Fus. Eng. Des. 24 (1994) 159.